Surface ocean carbon dioxide during the Atlantic Meridional Transect (1995-2013); evidence of ocean acidification.

Vassilis Kitidis[1,*], Ian Brown[1], Nicholas Hardman-Mountford[1,2], Nathalie Lefèvre[3]

1: Plymouth Marine Laboratory, PL13DH, United Kingdom

2: CSIRO Oceans & Atmosphere, Centre for Environment and Life Sciences, Floreat 6014, WA, Australia

3: IRD-LOCEAN, Sorbonne Universités (Université Pierre et Marie Curie-CNRS-MNHN), 4 place Jussieu, 75252 Paris Cedex 05, France

*: corresponding author (vak@pml.ac.uk)

Abstract

Here we present more than 21000 observations of carbon dioxide fugacity in air and seawater (fCO2) along the Atlantic Meridional Transect (AMT) programme for the period 1995-2013. Our dataset consists of 11 southbound and 2 northbound cruises in boreal autumn and spring respectively. Our paper is primarily focused on change in the surface-ocean carbonate system during southbound cruises. We used observed fCO2 and total alkalinity (TA), derived from salinity and temperature, to estimate dissolved inorganic carbon (DIC) and pH (total scale). Using this approach, estimated pH was consistent with spectrophotometric measurements carried out on 3 of our cruises. The AMT cruises transect a range of biogeographic provinces where surface Chlorophyll *a* spans two orders of magnitude (mesotrophic high latitudes to oligotrophic subtropical gyres). We found that surface Chlorophyll *a* was negatively correlated with fCO2, but that the deep chlorophyll maximum was not a controlling variable for fCO2. Our data show clear evidence of ocean acidification across 100 degrees of latitude in the Atlantic Ocean. Over the period 1995-2013 we estimated annual rates of change in: a) sea surface temperature of 0.01 ± 0.05 degrees C, b) seawater fCO2 of 1.44 ± 0.84 μatm, c) DIC of 0.87 ± 1.02 μmol per kg and d) pH of -0.0013 ± 0.0009 units. Monte Carlo simulations propagating the respective analytical uncertainties showed that the latter were < 5% of the observed trends. Seawater fCO_2 increased at the same rate as atmospheric CO_2.

Highlights

- Observations along the AMT track, over 19 years showed increase in seawater CO_2.
- Seawater CO_2 increase followed the respective atmospheric increase
- Ocean Acidification rate of 0.0013 units per year was observed
- Chlorophyll *a* was a major control of surface CO_2 along-track

---

Keywords

- Carbon dioxide; Carbonates; Greenhouse effect; Climatic changes; Acidification; Ocean acidification

---

Regional Index Terms

- Atlantic Ocean

1. Introduction

Carbon dioxide (CO_2) is a long-lived trace gas in the atmosphere contributing to the greenhouse effect. Atmospheric CO_2 has increased by approximately 45% since pre-industrial times due to anthropogenic emissions from fossil fuel combustion, cement production and land use changes. While CO_2 has been accumulating in the atmosphere, the oceans and land have acted as a sink over the same period taking up about half of anthropogenic CO_2 emissions (Le Quéré et al., 2015). Thereby, for the last decade, the oceans have taken up 29% of anthropogenic CO_2 emissions (Le Quéré et al., 2015). While this uptake moderates the accumulation of CO_2 in the atmosphere, and by extension global warming, the dissolution of CO_2 in seawater causes ocean acidification (OA) (Caldeira and Wickett, 2003).

Net CO_2 uptake by the oceans is controlled by the solubility and biological pumps. The former describes dissolution of CO_2 in seawater which is driven by the sea-air concentration gradient, the gas transfer velocity and solubility of CO_2 in seawater (a function of temperature and salinity). The biological pump describes the net uptake of CO_2 by biota and is controlled by the balance between photosynthesis and respiration which in turn determine the trophic status of the ocean (autotrophy vs. heterotrophy). The majority of anthropogenic C (C_{anth}) uptake to date is thought to be driven by the solubility pump. Thereby, in the Atlantic Ocean, C_{anth} uptake is largely restricted to surface waters (~400 m) with the exception of the North Atlantic where deep water formation transports C_{anth} to the ocean interior (Gruber, 1998; Orr et al., 2001; Wanninkhof et al., 2010). Deep-water formation in the north Atlantic is a critical component of the meridional overturning circulation (MOC). and constitutes the biggest oceanic sink for C_{anth} globally (Khatiwala et al., 2013).

Nevertheless, high spatial and temporal variability related to natural cycles is encountered across the Atlantic Ocean biogeochemistry. This is reflected in surface pCO_2 across different biogeographic provinces (Lefevre and Moore, 2000). The AMT programme, transects a number of these provinces from oligotrophic subtropical gyres to highly productive upwellings (Hooker et al., 2000). In the open ocean, at temperate latitudes along the AMT track, seasonal changes in photosynthesis and surface mixing result in high and highly-seasonal pCO_2 variability (Lefevre and Moore, 2000). Deep winter mixing entrains CO_2-rich deep water into the mixed layer leading to efflux of CO_2 to the atmosphere in winter, while the concomitant entrainment of nutrients enhances photosynthesis in spring/summer and drawdown of atmospheric CO_2 (Gruber et al., 2002). Coastal waters on the margins of the Atlantic Ocean are subject to terrestrial influences, tidal currents and show

greater short-term variability in pCO_2 than observed in the open ocean (Bianchi et al., 2005; Johnson et al., 2013; Marrec et al., 2013). The eastern margins of the Atlantic Ocean are dominated by upwelling systems: the Iberian, Mauritanian, Canary Current and Benguela upwellings. In these regions CO_2-rich deep water is upwelled resulting in efflux to the atmosphere, while the offshore transport of nutrients in upwelling filaments enhances photosynthesis and CO_2 drawdown (Gonzalez-Davila et al., 2009; Loucaides et al., 2012; Magdalena Santana-Casiano et al., 2009; Perez et al., 1999). The tropical Atlantic acts as a source of CO_2 to the atmosphere due to equatorial upwelling with some notable exceptions (Lefevre, 2009). Firstly, a persistent sink in the region of the inter-tropical-convergence zone (ITCZ; 5-8 ^{o}N) where low salinity increases the solubility of CO_2 (Lefevre et al., 1998). Secondly, a seasonal sink in the western tropical Atlantic driven by low salinity in the Amazon river plume (>40 ^{o}W) (Lefevre et al., 2010). The central North and South Atlantic, are dominated by the oligotrophic subtropical gyres where pCO_2 is generally close to equilibrium with the atmosphere (Lefevre and Moore, 2000).

The projected decrease in seawater pH under OA [up to 0.4 units by 2100 (Caldeira and Wickett, 2003; Feely et al., 2009)] is likely to impact biogeochemical cycles in the oceans, including calcification (Anthony et al., 2011), C-cycling (Riebesell et al., 2007) and N-cycling (Beman et al., 2011; Kitidis et al., 2011). It has been suggested that some genotypes of calcifying coccolithophores may be replaced by others which are able to compensate by calcifying more heavily (Beaufort et al., 2011). However, the ability to upregulate calcification has an associated energetic cost which may reduce the fitness of individuals (Wood et al., 2008).

Here, we focus on changes in pCO_2 and pH in surface waters of the Atlantic Ocean as sampled by the AMT programme between 1995 and 2013. There is recent evidence that the North Atlantic CO_2 sink may be decreasing in magnitude, though this may be part of natural variability. Long-term open ocean observations of CO_2 partial pressure (pCO_2) have shown that the magnitude of the North Atlantic sink is highly variable inter-annually driven by winter mixed layer depth variability (Bates, 2007; Gruber et al., 2002; Santana-Casiano et al., 2007; Schuster and Watson, 2007; Schuster et al., 2009). Progressive freshening of the North Atlantic over the last 50 years and into the future may slow the MOC critically (Curry and Mauritzen, 2005) and thereby impact on the capacity of the N. Atlantic to take up C_{anth}. Furthermore, time-series observations in the North Atlantic have revealed an increase in pCO_2 and concomitant decrease in pH, with the latter decreasing at -0.002 units annually (Bates, 2007; Bates et al., 2014; Lauvset and Gruber, 2014; Olafsson et al., 2009; Santana-

Casiano et al., 2007). In contrast, the South Atlantic is generally less well sampled with a recent study reporting an annual pH change of -0.001 (Lauvset et al., 2015).

2. Methods

2.1 Cruise programme

The AMT programme has covered 20 years of observations in the Atlantic Ocean since 1995 over nearly 100 degrees of latitude (Rees et al., 2015). The majority of cruises have taken place onboard the RRS James Clark Ross (JCR) on its annual southbound passage (September/November) from the UK to Antarctica. Northbound cruises in April/May were carried out predominantly in the early phase of the programme. More recently, AMT cruises have also taken place on the RRS James Cook and RRS Discovery. Opportunistic pCO_2 observations have also taken place in years when JCR has not hosted an AMT or on recent northbound cruises. Here we present pCO_2 results from 11 southbound and 2 northbound cruises (Table 1). Of these, 8 cruises have been part of the AMT programme and a further 3 have used the pCO_2 system on JCR whilst on-passage south (4 cruises) or north (1 cruise) along the AMT track. In total, 21280 pCO_2 observations were made over 19 years.

Table 1: List of cruises presented here. Cruises denoted A# were part of the AMT programme (where # denotes the AMT number). Cruises denoted J#N or J#S denote opportunistic observations from RRS JCR along the AMT cruise track (north- and south-bound respectively; where # denotes the year). Direction denotes southbound (S) or northbound (N) and the number of pCO_2 observations per cruise is (n).

Cruise	Direction (n)	Ship	Start	End
A1 (AMT 1)	S (455)	JCR	21/9/1995	24/10/1995
A2 (AMT 2)	N (254)	JCR	22/4/1996	28/5/1996
A3 (AMT3)	S (1931)	JCR	16/9/1996	25/10/1996
A7 (AMT7)	S (1805)	JCR	14/9/1995	25/10/1998
J07S	S (648)	JCR	24/9/2007	23/10/2007
J10S	S (932)	JCR	1/10/2010	24/10/2010
A20 (AMT20)	S (1017)	James Cook	12/10/2010	25/11/2010
J11N	N (775)	JCR	30/4/2011	25/5/2011
J11S	S (1565)	JCR	27/9/2011	19/10/2011
A21 (AMT21)	S (6349)	Discovery	29/9/2011	14/11/2011
J12S	S (114)	JCR	12/10/2012	8/11/2012
A22 (AMT22)	S (1758)	James Cook	10/10/2012	24/11/2012
A23 (AMT23)	S (3677)	JCR	5/10/2013	8/11/2013

The ships stopped for one or two daily hydrocasts (usually pre-dawn and at solar noon), during which seawater was collected from the upper 300 m of the water column for various biogeochemical observations and experiments.

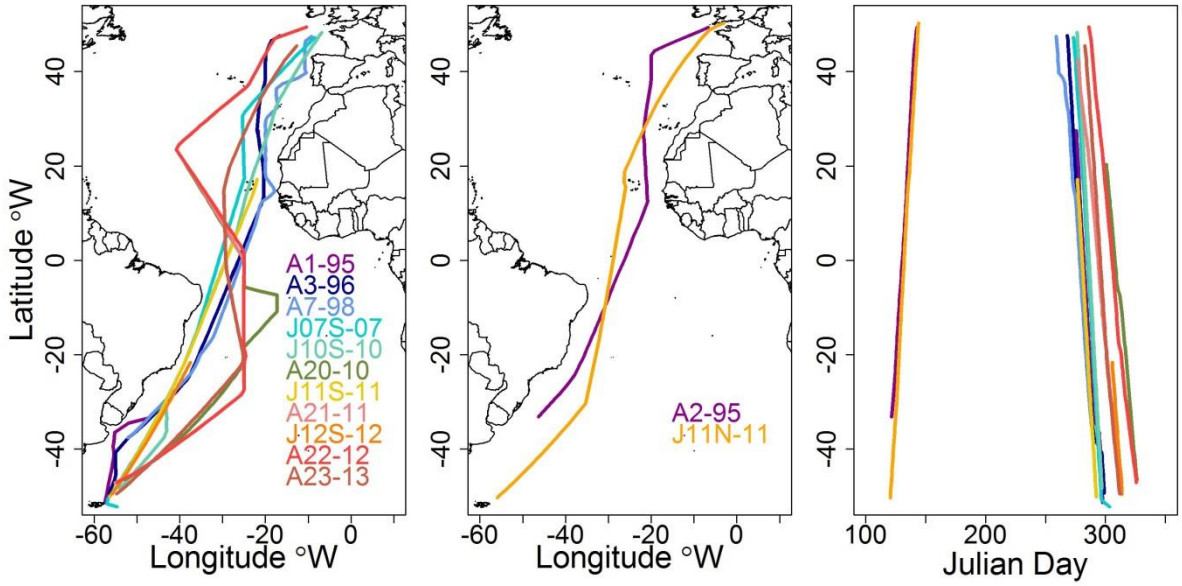

Figure 1: Cruise tracks for southbound cruises (left), northbound (middle) and the respective latitude versus Julian day (right; noon on 1st January is Julian Day 1.5). Cruise names are followed "- ##" denoting the year (e.g. A1-95 was in 1995; see Table 1 for exact dates)

2.2 CO_2 fugacity observations

Between 1995 and 1998 an autonomous CO_2 system was deployed encompassing a non-dispersive infrared detector (LiCor, Li6262), percolator-type equilibrator, mechanical and electronic hardware (Cooper et al., 1998). The system was calibrated using commercial CO_2 standards referenced to World Meteorological Organization primary standards (Cooper et al., 1998). The uncertainty of the system deployed in the period 1995-1998 was estimated as 1-2 µatm, during laboratory tests (Lefevre et al., 1998).

From 2007 onwards an evolution of this system, the PML-Dartcom *Live*pCO_2 system was deployed. The system encompasses a non-dispersive infrared detector (LiCor, Li840), showerhead equilibrator (vented through a parallel second equilibrator), Peltier-dryer, gas-sampling and electronics hardware. The system was connected to the underway-seawater flow and set up to sample every 20 minutes. The intake of the ship's underway-seawater system is located at approximately 7 m depth for all three ships. The *Live*pCO_2 system was calibrated using secondary CO_2 standards every hour (BOC gases Ltd; nominal 0, 250 and

450 ppmv CO_2 in synthetic air). In turn, these were calibrated against NOAA-certified primary reference standards (National Oceanic and Atmospheric Administration; 244.9 and 444.4 ppmv CO_2). Between 2007 and 2010, the system was fitted with a single 'closed loop' equilibrator which was prone to equilibration-headspace pressure changes (Kitidis et al., 2012). This effect was ship-specific and was not found to affect the system installed on RRS JCR (i.e. the data presented here). Laboratory inter-comparison tests showed that our system was in agreement with independent, similar systems (within ±0.5 µatm). An at-sea inter-comparison of the JCR system in 2008 showed agreement with an independent system within ±3 µatm (Jones et al., 2012). The 2010-onwards setup (with the vented equilibrator) was tested during a separate at-sea inter-comparison exercise against independent measurements of fCO_2 and other carbonate system parameters (TA, DIC, pH) with an accuracy of ±4 µatm (Ribas-Ribas et al., 2014). It should be noted that the latter was equivalent to the analytical uncertainty of fCO_2 derived from TA/DIC/pH (e.g. typical uncertainty of ±2 µmol L^{-1} for DIC is equivalent to ±4 µatm fCO_2 at 20 ^{o}C and salinity 35).

Data reduction followed standard best practices (Dickson et al., 2007). Data are reported as CO_2 fugacity (fCO_2) rather than partial pressure in order to account for the non-ideal behaviour of CO_2. The sea-air difference in CO_2 fugacity (ΔfCO_2) was calculated by subtracting seawater fCO_2 ($fCO_{2\ sea}$) from concurrent atmospheric measurements ($fCO_{2\ air}$).

2.3 Carbonate observations

The concentrations of individual species of a CO_2-in-water solution can be determined by knowing two of the four parameters of the carbonate system (fCO_2, DIC, TA and pH). As CO_2 dissolves-in and reacts with water, it forms carbonic acid which further dissociates to carbonate and bicarbonate. The sum of these terms is called Dissolved Inorganic Carbon (DIC). Total Alkalinity (TA) is defined as the number of moles of hydrogen ion equivalents in excess of proton acceptors. Finally, pH is defined as negative $\log_{10}$ of hydrogen ion concentration. During AMT 22 (cruise A22), samples were collected for TA/DIC from the daily hydrocasts. Further samples were collected for spectrophotometric pH analyses on AMT21, AMT22 and AMT23. Typically, 3 samples per cast were collected for TA/DIC (surface, DCM and deepest Niskin bottle) and 11 samples per cast for pH (focusing primarily at SML and pycnocline). TA/DIC samples were collected in 250 mL clear glass bottles straight from the Niskin bottles using dilute-HCl-cleaned Si-tubing and preserved using 100 µL of saturated $HgCl_2$ solution. The bottles were sealed with glass stoppers which were lightly greased using Apiezon H grease (Sigma-Aldrich, Z273562-1EA). The samples were

stored until analysis in the laboratory (within 12 months). DIC samples were analysed using an Apollo SciTech AS-C3 DIC analyser. The analyser draws a pre-defined volume of sample which is acidified with H_3PO_4 to convert all DIC into CO_2 which is sparged with N_2 and passed through a solid state infrared detector (LiCor, LI7000). TA was analysed immediately following DIC analysis using an Apollo SciTech AS-ALK2 analyser. The instrument follows an open-cell-titration of a known volume of sample to pH 3 using HCl (Dickson et al., 2007). DIC and TA measurements were calibrated using certified reference materials from the Scripps Institute of Oceanography (A.G. Dickson; batch 126 and 127). The precision and accuracy of replicate CRM analyses were better than ±2 μmol L^{-1} (n=6). pH was determined spectrophotometrically onboard the ship using the m-cresol-purple dye (Clayton and Byrne, 1993). The dye has two absorbance maxima at 434 nm and 578 nm, the ratio of which is pH-, temperature- and salinity dependent. Samples were collected from the Niskin bottles using dilute-HCl-cleaned Si-tubing and placed in a water bath at 25 ^{o}C. 100 μL of dye were added to 35 mL of sample and absorbance was recorded on a spectrophotometer (Perkin Elmer, Lamda 35). The measurement temperature was recorded using a National Institute of Standards and Technology -traceable thermometer (VWR, VWRI620-2000). Sample salinity was taken from the conductivity temperature depth sensor (CTD) on the hydrocast (see below). Absorbance readings were corrected for the pH-change caused by the addition of the dye and pH is reported on the "Total" activity scale (pH_T) (Dickson et al., 2007). The precision of triplicate pH_T samples was ±0.001 units or better (triplicate samples were analysed on 17 occasions).

In order to extend our data, we used a generic function of salinity and temperature to obtain a best fit for our TA data (Lee et al., 2006). The fit is given by equation 1:

$$TA = 2305 + 53.97(S - 35) + 2.74(S - 35)^2 - 1.16(T - 20) + 0.04(T - 20)^2 \quad (1)$$

where T is the temperature and S is the salinity of the samples.

2.4 Other observations (Temperature, Salinity, Chlorophyll).

Sea surface temperature (SST), temperature at depth and salinity were recorded with a thermosalinograph underway and a conductivity temperature depth (CTD) instrument on the hydrocast (Sea-Bird Electronics, models: ocean logger / SBE45 / 9plus). Salinity was calibrated by discrete bottle sample analysis (Guildline, model: Autosal) using IAPSO standards. Temperature on the hydrocast was calibrated by discrete reversing thermometers (Sensoren Instrumente Systeme) until 1998. Subsequently, calibration of the platinum resistance thermometers was undertaken annually by the manufacturer. Discrete Chlorophyll

a samples were collected underway and at depth using the Niskin bottles on the hydrocast and analysed fluorometrically following acetone extraction (Welshmeyer, 1994). Briefly, Chlorophyll samples were filtered through 0.7 μm GF/F filters and placed in acetone for 18-36 hours before fluorescence was measured (Turner Designs, AU10 fluorometer). Post 1996 (AMT3 onwards), these samples were used to calibrate a fluorometer on the hydrocast sensor package. For each AMT hydrocast station (designation A* in Table 1), the depth of the surface mixed layer (SML) was computed as the depth where the derivative of σ_T (σ_T is defined as seawater density – 1000 kg m^{-3}) ($\partial(\sigma_T)/\partial(Z)$, where Z is water depth in m) exceeded 0.01 m^{-1} and 0.04 m^{-1}. The former criterion identified short-term stratification of the water column (days to weeks), while the latter identified seasonal stratification over longer time scales (months).

2.5 Carbonate system internal consistency and trend uncertainty

The fit of TA predicted by equation 1 ($TA_{predicted}$) against measurements is shown in Figure 2. We used $TA_{predicted}$ and fCO_2 to calculate $pH_{T\ predicted}$ for surface samples collected during AMT21-23 using CO2SYS software (.xls; v.14) (Lewis and Wallace, 1998) using the H_2SO_4 dissociation constants of Dickson et al. (Dickson, 1990) and the carbonic acid dissociation constants of Millero et al. (Millero et al., 2006). The calculated $pH_{T\ predicted}$ values were significantly correlated with pH_T measurements on the three AMT cruises (Pearson R^2=0.94, p<0.001, df=184) with a slope and intercept indistinguishable from 1 and 0 respectively (slope = 1.02 ± 0.02 and intercept = -0.2 ± 0.2) (Figure 2). The standard error of residuals was 0.0056 pH units. This internal consistency of a derived independent variable with measurements across three independent cruises gives us confidence to apply equation 1 across our dataset and calculate $TA_{predicted}$ for all cruises. The combination of fCO_2 and $TA_{predicted}$ gives two of the four carbonate system parameters required to calculate the remaining two, here DIC and pH_T. For selected surface samples on AMT22, we thereby had all four carbonate system parameters (DIC,TA, pH_T and pCO_2). All possible pairs of these were used to calculate the remaining pair and found to be consistent with observations.

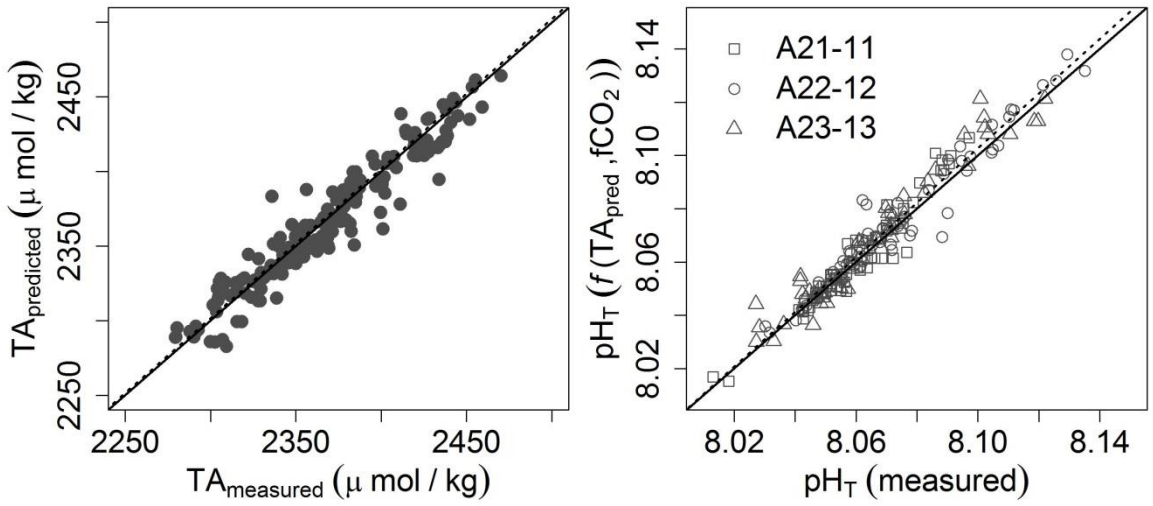

Figure 2: TA predicted from equation 1 versus measurements on AMT22 (left; $TA_{predicted}$=1.00±0.02 × $TA_{measured}$ - 6±49) and pH_T calculated from $TA_{predicted}$ and fCO_2 against measurements on AMT21, AMT22 and AMT 23 (right; $pH_{T\ predicted}$=1.02±0.02 × $pH_{T\ measured}$ -0.2±0.2). Dashed lines represent the respective regression lines while solid lines represent the 1:1 line.

Our analysis of $fCO_{2\ sea}$ and pH_T trends includes analytical uncertainty which may bias their respective trends. As stated above, the analytical uncertainty for $fCO_{2\ sea}$ was ±4 μatm which is equivalent to ±0.0035 pH_T units at the mean SST and salinity for our dataset. Potentially larger sources of uncertainty are a) the analytical uncertainty of TA, b) uncertainty arising from equation 1 for $TA_{predicted}$ and c) uncertainty arising from the calculation of $pH_{T\ predicted}$ (using CO2SYS). The combined effect of the latter uncertainties on pH_T is captured by the standard error of the regression for $pH_{T\ predicted}$ (±0.0056 units; see above and Figure 2).

In order to estimate the effect of the $fCO_{2\ sea}$ and $pH_{T\ predicted}$ analytical uncertainties (±4 μatm and 0.0056 units respectively) on the respective trends we carried out a Monte Carlo uncertainty propagation. We used the '*jitter*' function in R to introduce random noise to our data (within 4 μatm and 0.0056 units respectively). As the noise introduced was by definition 'random', we ran 10^3 iterations of the script, in order to ensure representative results. The mean trend for each 1-degree data-bin ($fCO_{2\ sea}$ data) including this random noise was statistically indistinguishable from the corresponding observations [paired T-test, n=99, the mean p-value of 10^3 iterations of 'random noise addition' was 0.50±0.29]. Similarly, the mean trend in pH_T for each 1degree data-bin including this random noise was statistically indistinguishable from the corresponding observations [paired T-test, n=99, the mean p-value of 10^3 iterations of 'random noise addition' was 0.49±0.29].

Subsequently, we performed a kernel density estimation (KDE) on the 10^3 mean $fCO_{2\ sea}$ and pH_T trend-estimates using a Gaussian fit ('*density*' function in R). From the KDE we computed the respective 95 % confidence intervals for the effect of random noise addition on the mean trends. The corresponding density histograms are shown in (Figure 3) and the 95 % confidence intervals for the contribution of the analytical errors to the $fCO_{2\ sea}$ and pH_T trends from this analysis were ±0.05 µatm and $\pm 7 \times 10^{-5}$ pH units respectively (or < ±5 % of the observed trends). These 'random' analytical errors thereby cancelled each other out when computing the respective trends. We are therefore confident that the $fCO_{2\ sea}$ and pH_T analytical and calculation errors did not bias our results regarding observed trends in $fCO_{2\ sea}$ and pH_T.

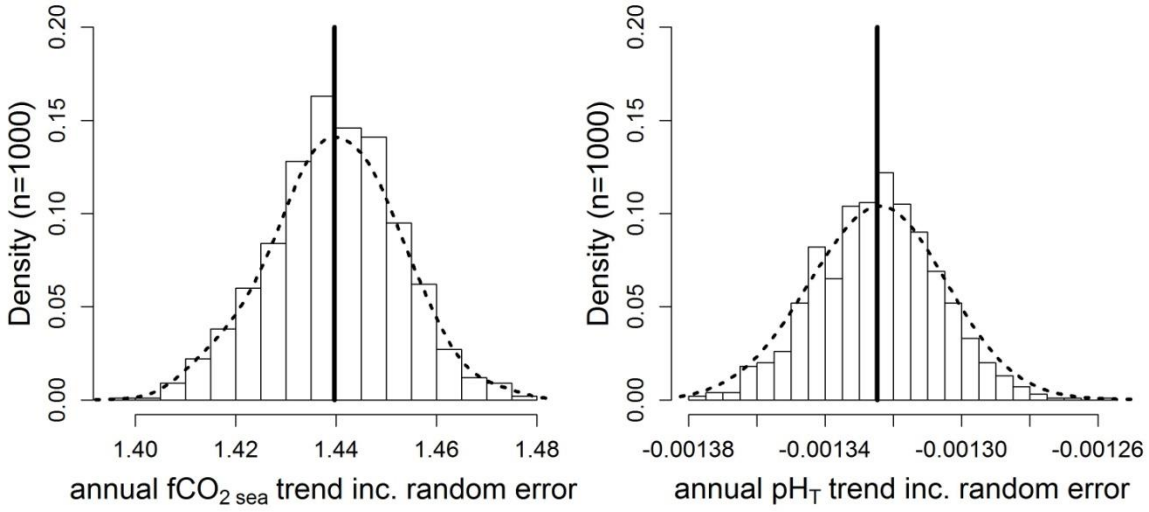

Figure 3: Density histogram of mean annual $fCO_{2\ sea}$ (left) and pH_T trends (right). Random noise (within the analytical uncertainty) was added to each of 10^3 iterations used here. Solid vertical lines represent the observed trends and dashed lines represent the Gaussian fit from the kernel density estimation.

2.6 Multiple linear regression: fCO_2 and ΔfCO_2

In order to identify the main controls on $fCO_{2\ sea}$ we carried out a multiple linear regression (MLR) analysis in R (version 3.1.2). The rationale was to build an MLR model with the least number of input variables, where SST, Salinity and $fCO_{2\ air}$ determine the physical dissolution of CO_2 in seawater (physical controls), while Chlorophyll *a* represents biological controls of CO_2 (as a first order approximation). A further variant of the MLR used depth integrated Chlorophyll *a*, using a dynamic maximum depth of integration (defined as ∂(Chlorophyll *a*)/∂(depth)< standard deviation over the deepest 10 m of each cast). However,

this was found to covary with surface Chlorophyll *a* here and is therefore not discussed further. All MLR analysis was carried out on AMT cruises only (designation A* in Table 1) and from AMT3 onwards when a continuous fluorometric-sensor was fitted to the hydrocast. In total, 308 hydrocast profiles were processed in R and used in the MLR analysis.

3. Results

The water column typically exhibited stratification with a surface mixed layer (SML) which is more pronounced in the subtropical gyres (up to 135 m and 186 m in depth in the northern and southern sub-tropical gyres respectively). At the base of the SML, a deep chlorophyll maximum (DCM; 120 m and 150 m in the northern and southern gyres respectively) and O_2 maximum ($O_{2\ max}$; 80 m and 90 m in the northern and southern gyres respectively) are typically found. At higher latitudes (north of 40 ^{o}N and south of 40 ^{o}S), highest chlorophyll and O_2 are observed near the surface (5-30 m in depth). For logistical and scientific reasons, the cruise tracks have varied over the last two decades (Smyth et al., submitted) (Figure 1). Therefore, it is important to note that some changes in pCO_2 over this period may be ascribed to track- or timing-variations. This is discussed in further detail below.

Salinity, surface Chlorophyll-α concentration (Chl_{surf}), atmospheric $fCO_{2\ air}$, seawater $fCO_{2\ sea}$ and ΔfCO_2 are shown in Figure 4 (southbound) and Figure 5 (northbound; $fCO_{2\ air}$, $fCO_{2\ sea}$ and ΔfCO_2 only) as averages in 1 degree of Latitude bins. The salinity distribution reflects the balance between freshwater inputs and evaporation, highlighting the North Atlantic and South Atlantic subtropical gyres (NAG: 25-40 ^{o}N and SAG: 15-30 ^{o}S respectively) where high salinity is typically found during AMT. Conversely, the subtropical gyres are characterised by low surface Chlorophyll-α concentration. In the equatorial region, high precipitation in the Inter Tropical Convergence Zone (ITCZ) reduces salinity, while equatorial upwelling supplies nutrients which fuel higher Chl_{surf}. $fCO_{2\ air}$ increased over the period of observations by 30-40 µatm (1995-2013). $fCO_{2\ sea}$ showed a similar increase in our data, although there is considerably more noise, particularly at higher latitudes along the cruise tracks. $fCO_{2\ sea}$ and ΔfCO_2 showed a remarkably consistent distribution pattern with latitude in agreement with an earlier study describing the latitudinal distribution of fCO_2 for AMT1-3 (Lefevre and Moore, 2000). Thereby, at high latitudes (north of 40^{o}N and south of 30 ^{o}S), surface waters were generally undersaturated with respect to atmospheric equilibrium (negative ΔfCO_2). The North Atlantic subtropical gyre (NAG: 25-40 ^{o}N) was oversaturated in boreal autumn (southbound cruises) and undersaturated in boreal spring (northbound cruises).

The South Atlantic subtropical gyre (SAG: 15-30 ^{o}S) was undersaturated or in equilibrium in both spring and autumn. The region of 10-25 ^{o}N was oversaturated in boreal autumn, and over- / under-saturated in spring 1996 and 2011 respectively. The region of the NECC, North Equatorial Counter-Current (3-10 ^{o}N) (the ITCZ is at its southernmost position south of the equator (0-2^{o}S) in March and migrates seasonally to reach about 10^{o}N in July) was generally undersaturated in boreal autumn and in equilibrium with the atmosphere in boreal spring. The equatorial region and transition to the SAG (2 ^{o}N -15 ^{o}S) was generally oversaturated in both spring and autumn.

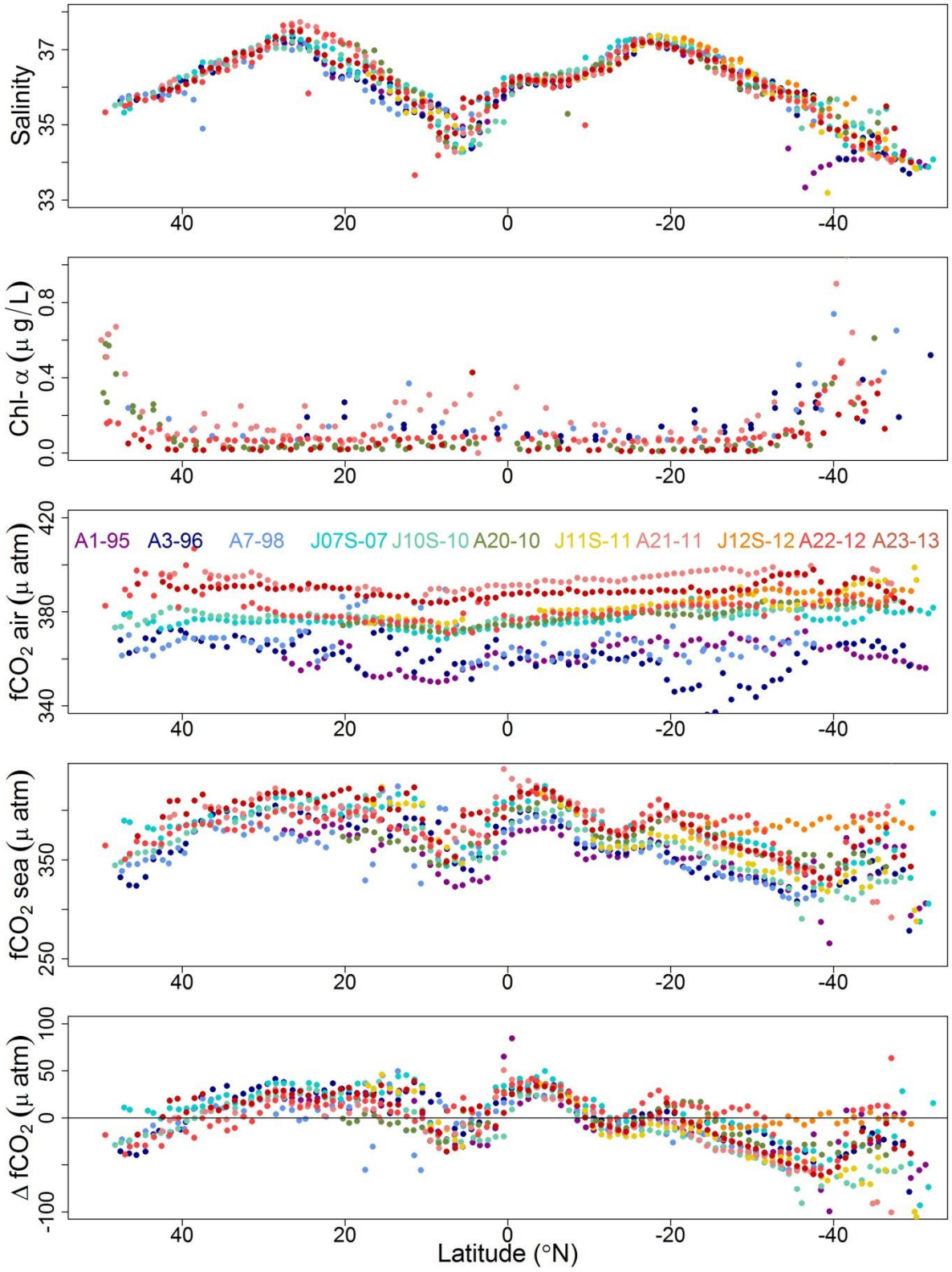

Figure 4: Salinity, Chlorophyll-α, CO_2 fugacity in air, seawater fCO_2 and ΔfCO_2 against latitude for southbound cruises in boreal autumn. Negative ΔfCO_2 in bottom panel denotes undersaturation of surface seawater with respect to atmospheric equilibrium.

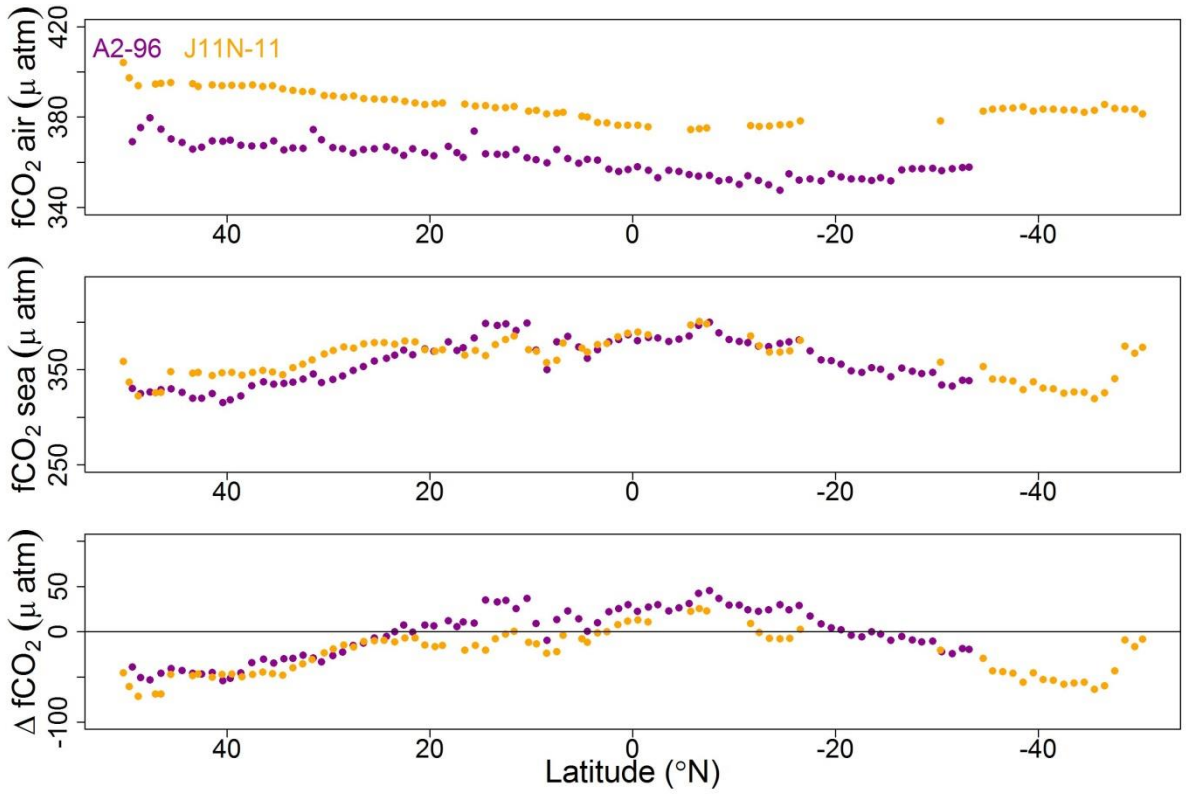

Figure 5: CO_2 fugacity in air (top), seawater (middle) and sea-air difference (bottom) for northbound cruises in boreal spring. Negative ΔfCO_2 in bottom panel denotes undersaturation of surface seawater with respect to atmospheric equilibrium.

In order to determine rates of change over the 19 years covered by our observations, we grouped data from each cruise into 1 degree of latitude bins. The slope of each parameter with time was then calculated for each bin (e.g. $fCO_{2\ sea}$ vs. Year in 12-13 ^{o}N bin). This analysis was limited to southbound cruises (n=11) since the limited number of northbound cruises (n=2) would not give a statistically significant trend. The rate of $fCO_{2\ sea}$ change in each latitudinal bin is shown in Figure 6. Atmospheric $fCO_{2\ air}$ increased by 1.47±0.35 µatm y^{-1} over the 19 years covered by our cruises. Seawater $fCO_{2\ sea}$ from our data increased by 1.44±0.84 µatm y^{-1} (Figure 6). The mean rate of $fCO_{2\ sea}$ increase for 1 degree of latitude binned data was statistically indistinguishable from the respective mean rate of $fCO_{2\ air}$ increase (paired T-test, p=0.679, n=99). The increase in surface seawater CO_2 therefore followed the increase in atmospheric CO_2. Nevertheless, there were regional exceptions to this, notably between 30-35 ^{o}N, 7-12 ^{o}N and south of 40 ^{o}S. These exceptions may be due to cruise track differences, where the early cruises followed a more westerly track passing closer to the Canary- and Mauritanian-upwelling systems where one may expect higher fCO_2. Nevertheless, this was not reflected in SST or salinity. Park and Wanninkhoff found that winter $fCO_{2\ sea}$ did not follow the atmospheric increase in the Caribbean Sea and attributed

this to changes in SST and mixed layer depth via climatic forcing (Park and Wanninkhof, 2012). In our study, we did not observe changes in SST or MLD in the regions of low $fCO_{2\ sea}$ increase. As expected, the mean rate of ΔfCO_2 change was not significantly different from zero (mean ΔfCO_2 = -0.03±0.82 μatm y^{-1}, T-test, p=0.679, df=99) (Figure 6). The mean rate of DIC change was 0.87±1.02 μmol kg^{-1} y^{-1} and was significantly different from zero (T-test, p<0.001, df=99). The respective mean rate of $pH_{T\ predicted}$ change (see section 2.3) was –0.0013±0.0009 units y^{-1} (Figure 6) and was significantly different from zero (T-test, p<0.001, df=99). A mean warming trend of 0.04±0.10 ^{o}C y^{-1} was found for SST, but this was heavily biased by high apparent warming north of 38 ^{o}N. In this northernmost subset of our data there may be a bias introduced by cruise track and/or timing between early cruises (1995-1998) and later cruises (2010 onwards). The latter generally followed a more westerly track north of 38 ^{o}N. Excluding these data gave a mean SST warming of 0.01±0.05 ^{o}C y^{-1}. Both SST trends were statistically different from zero (T-test, p<0.001 and p<0.022 for df=99 and df=85 respectively).

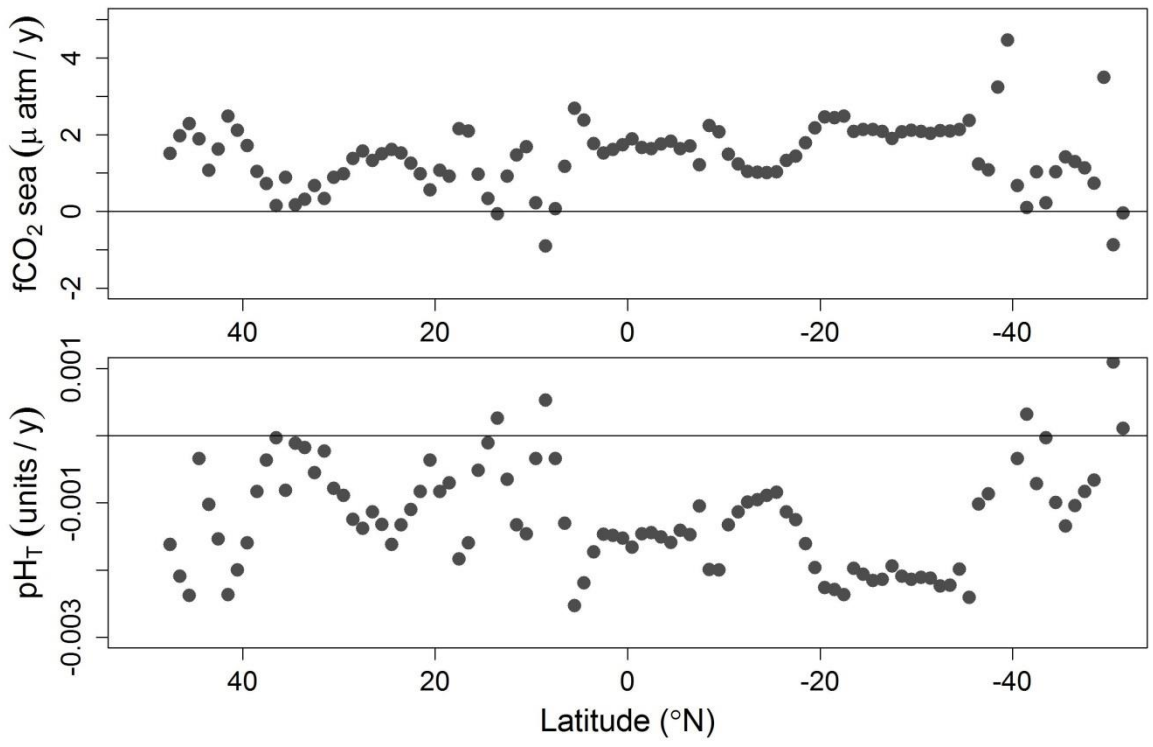

Figure 6: Annual rate of change in CO_2 fugacity in seawater ($fCO_{2\ sea}$) and annual rate of pH_T change (bottom) for southbound cruises in boreal autumn.

In the context of 'change' over this period, it is important to firstly consider differences in cruise track and timing in order to identify any potential bias these may cause. For

example, a closer examination of the cruise tracks in Figure 1 shows that AMT20-22 (in 2010-2012) followed a more westerly track at these northern latitudes. These cruises would have entered the subtropical north Atlantic gyre earlier (and at higher latitude) where higher SST would be expected. Given that these cruises took place towards the latter part of our study, this may be a source of bias when estimating trends in our dataset. South of 38 ^{o}N, we observed a mean SST increase of 0.01 ^{o}C y^{-1}. In contrast the overall SST warming trend (0.04 ^{o}C y^{-1}), likely reflects some cruise track bias north of 38 ^{o}N. Based on CO_2 solubility calculations (Weiss, 1974), the corresponding annual change in $fCO_{2\ sea}$ would be +0.1 µatm y^{-1} (for a 0.01 ^{o}C annual increase in SST). Since the observed increase in $fCO_{2\ sea}$ exceeds the effect of SST by one order of magnitude, we are confident that the latter does not substantially bias the trend in fCO_2 reported here. In order to further test the potential bias of different cruise tracks we compared the surface mixed layer (SML) and DCM depth across southbound AMT tracks. Our rationale for doing this was that if $fCO_{2\ sea}$ was influenced by track on particular cruises (e.g. upwelling filaments for more easterly tracks in the North Atlantic), then this influence would also manifest itself in the SML- and DCM-depths. Therefore, data were binned into 1 degree of latitude subsets and a linear fit of SML depth against time was applied to each subset. This analysis showed that the rate of change in SML depth was not statistically significant from zero for either $\partial(\sigma_T)/\partial(Z)$=0.01 m^{-1} or $\partial(\sigma_T)/\partial(Z)$=0.04 m^{-1} (T-test, p>0.05, n=83 in both cases). There was also no significant change in the depth of the DCM, surface Chlorophyll *a* or Chl_{DCM} (T-test, p>0.05, n=83). Overall therefore we are confident that the track- and timing-differences of our cruises did not bias our results.

The MLR model used to identify controls of $fCO_{2\ sea}$ is given by:

$$fCO_{2\ sea} = fCO_{2\ air} + 2.6SST + 6.4S - 8.8\ Chl_{surf} \quad (R^2 = 0.51) \qquad (2)$$

ΔfCO_2 showed a weaker correlation coefficient (R^2=0.44). In both models $fCO_{2\ sea}$ was strongly and positively correlated with $fCO_{2\ air}$, SST and salinity. Concurrently, $fCO_{2\ sea}$ was negatively correlated with surface Chlorophyll *a*. ΔfCO_2 followed the same pattern as $fCO_{2\ sea}$ in both models with the exception of $fCO_{2\ air}$ which was not significant.

4. Discussion

In this paper we focus on change in CO_2 fugacity (fCO_2), the air sea fugacity gradient (ΔfCO_2) and pH_T of surface waters along the AMT track over a period of 19 years. In this context, it is important to establish that our observed changes in the carbonate system were indeed related to time and not analytical uncertainty or differences in cruise track. Random

error propagation, within the boundaries of combined analytical and calculation uncertainties, showed that the effect of these uncertainties on the trends of $fCO_{2\ sea}$ and pH_T were less than 5 % of the observed trends (see section 2.5). The effect of cruise track variability is more complex. The apparent SST warming trend of 0.01 $^{o}C\ y^{-1}$ (excluding data north of 38 ^{o}N) was consistent with the 1979-2012 trend reported by the Intergovernmental Panel on Climate Change (Hartmann et al., 2013). It is also in agreement with the work of Aiken et al. presented in this issue. The absence of significant differences in SML and DCM depth as well as Chl_{surf} and Chl_{DCM}, further corroborate our assumption that cruise track variability did not bias our carbonate data and their interpretation.

For a given atmospheric CO_2 concentration, ΔfCO_2 can be affected by gas exchange, changes in solubility (a function of temperature and salinity) or biological activity (photosynthesis and respiration). Lateral transport and entrainment of deep water further determine $fCO_{2\ sea}$ and by extension ΔfCO_2. Where ΔfCO_2 is negative, surface waters are undersaturated with respect to equilibrium with the atmosphere, suggesting a source-sink imbalance. Net community production (NCP=photosynthesis-respiration) is frequently used to assess the net trophic status of the ocean (autotrophic vs. heteroptrophic). Dissolved CO_2 in seawater is, to a certain extent, buffered against gas-exchange by the carbonate system. Therefore, unlike other gases, such as O_2, which have a surface mixed layer turnover time of days to weeks (through gas exchange), the turnover time of CO_2 is in the order of months (Broecker and Peng, 1974). Thereby, ΔfCO_2 retains a 'memory' of various processes, integrated over this timescale, such as NCP, particularly in regions such as the subtropical gyres where advective processes play a minor role.

The distribution of $fCO_{2\ sea}$ and its sea-air difference (ΔfCO_2) observed here were consistent with previous AMT studies and the broader distribution of biogeographic provinces (Hooker et al., 2000; Lefevre and Moore, 2000). In order to avoid repetition, the reader is referred to these publications regarding the detailed distribution of $fCO_{2\ sea}$ and ΔfCO_2 along biogeographic provinces sampled by the AMT programme. Nevertheless, it is useful to make some broad observations on our 13-cruise dataset.

Firstly, the broad distribution of salinity with latitude consistently showed high salinity in the subtropical gyres with lower values in temperate latitudes and around the equator (Figure 3). Low salinity in the region of 5-10 ^{o}N, reflected high precipitation related to the Intertropical Convergence Zone (ITCZ). Surface Chlorophyll *a* (Chl_{surf}) was lowest in the subtropical gyres whilst higher Chl_{surf} was found in temperate waters and the equatorial

region where this coincided with carbon dioxide undersaturation (negative ΔfCO_2). These distribution patterns (Chl_{surf} and ΔfCO_2) were consistent with the distribution of productivity which is highest in mesotrophic temperate- and equatorial-waters along the AMT track (Serret et al., 2015; Tilstone et al., 2015). In contrast, near-equilibrium ΔfCO_2 was observed in the subtropical gyres consistent with lower productivity.

Secondly, given the slow turnover of CO_2 (via gas exchange), it is possible to infer on the trophic status of the open ocean from ΔfCO_2 data (Juranek et al., 2012). The topic of net autotrophy versus net heterotrophy in the open ocean is currently the subject of intense debate in the literature (Duarte et al., 2013; Williams et al., 2013). From our data, the north Atlantic gyre (NAG) showed a clear seasonal pattern with oversaturation in boreal autumn and undersaturation in boreal spring consistent with uptake of CO_2 by phytoplankton in spring (Bates, 2007). In contrast, ΔfCO_2 in the south Atlantic subtropical gyre (SAG) appears to be near equilibrium in austral autumn and undersaturated in austral spring. This difference between the two gyres is also reflected in AMT NCP data which show that the south Atlantic gyre is more frequently autotrophic while the northern gyre is in trophic balance or heterotrophic (Serret et al., 2015). While the in-vitro work of Serret et al. (2015) gives an instantaneous measure of NCP, ΔfCO_2 may give an integrated measure of NCP over longer time scales similar to geochemical measures of NCP. The inference of trophic status from ΔfCO_2 may be somewhat speculative, but is nevertheless consistent with previous work.

Thirdly, physical controls have a strong influence on $fCO_{2\ sea}$ and hence ΔfCO_2 along the AMT track. For example, negative ΔfCO_2 in the NECC is consistent with this region acting as a sink for atmospheric CO_2 due to low salinity which in turn increases the solubility of CO_2 (Lefevre et al., 1998). Local hydrography also played a major part. For example, in the South Equatorial Current (1 ^{o}N to 15 ^{o}S) ΔfCO_2 was persistently positive, consistent with equatorial upwelling and advection of CO_2 rich waters from depth as well as the Benguela Upwelling system further East (Hooker et al., 2000). The major influence of physical and biological controls was also highlighted by our multi linear regression analysis (MLR).

The MLR analysis clearly identified SST and salinity as highly significant predictor variables for $fCO_{2\ sea}$ (equation 2). The purpose of this analysis was to obtain qualitative rather than quantitative information. Differences in the turnover times of these variables precluded a more quantitative assessment. For example, the turnover time of Chlorophyll *a* may be days to weeks compared to months for $fCO_{2\ sea}$, so that low $fCO_{2\ sea}$ may persist for some time after a phytoplankton bloom has collapsed. In this study, surface Chlorophyll *a*

was significantly and negatively correlated with $fCO_{2\ sea}$ (Equation 2) as one would expect from the drawdown of CO_2 by phytoplankton. Nevertheless, it is important to consider the limitations of using Chlorophyll *a* as a proxy for NCP or phytoplankton biomass here. While this is arguably a valid assumption as a first-order approximation along large productivity gradients (as sampled by AMT), the phytoplankton C: Chlorophyll *a* ratio is known to vary between species, with depth, light-field and nutrient status (Geider, 1987; Geider et al., 1998). It follows therefore that the Chlorophyll *a* – biomass relationship will also be variable. A direct measure of productivity (NCP or $^{14}C\text{-}HCO_3^-$ uptake) may therefore be a better predictor of $fCO_{2\ sea}$, but this is beyond the remit of this paper.

The increase in atmospheric CO_2 fugacity observed here (30-40 µatm) was consistent with the global mean atmospheric CO_2 increase of ~37 µatm over the same period, as measured by flask data (http://www.esrl.noaa.gov/gmd/ccgg/trends/). The concomitant increase in $fCO_{2\ sea}$ followed the atmospheric CO_2 increase over the 19-year period examined here (1995-2013). Indeed, the slope of $fCO_{2\ sea}$ versus $fCO_{2\ air}$ from the MLR (Equation 2, slope ~ 1.0) shows that an increase in atmospheric CO_2 was strongly correlated with a near-equal increase in seawater CO_2. This is further in agreement with the rate of change of $fCO_{2\ sea}$ and $fCO_{2\ air}$ between 1995 and 2013 in our data (1.44±0.84 µatm y^{-1} and 1.47±0.35 µatm y^{-1} respectively). Consequently, ΔfCO_2 has not changed significantly here (rate=-0.03±0.82 µatm y^{-1}). This implies that other processes controlling CO_2 in seawater have not changed over the period of 1995-2013 or that they have cancelled each other out. This does not contradict our earlier conclusion that the observed increase in SST would lead to an increase in $fCO_{2\ sea}$ of 0.1 µatm y^{-1} since the latter is within the uncertainty of the overall trend in $fCO_{2\ sea}$. Other processes controlling $fCO_{2\ sea}$ include NCP as well as local hydrography which may advect CO_2. Our data suggest that the increasing seawater-uptake of CO_2 across the Atlantic Ocean was largely driven by increasing atmospheric CO_2 through physical dissolution (gas exchange) and not enhanced uptake by biota. Nevertheless, satellite observations suggest that primary production may be decreasing over certain parts of the Atlantic Ocean (Tilstone et al., 2009). If so, then a concomitant decrease in respiration would also have to take place in order to maintain NCP and ΔfCO_2.

In order to determine the effect of increasing $fCO_{2\ sea}$ on the carbonate system of surface waters here, we used the $fCO_{2\ sea}$ data and TA, derived from salinity and SST. In the first instance, an increase in $fCO_{2\ sea}$ would be expected to lead to an increase in DIC and reduction in pH_T. While the inclusion of SST in the calculation of TA improves the fit across

different water masses (compared to a fit of TA against salinity only) (Lee et al., 2006), this also introduced an artificial temperature-dependence (equation 1) as TA is temperature-independent. In order to quantify this potential error we used the apparent warming trend from our data and found that our calculated TA would decrease by 1.84 μmol kg^{-1} over 19 years using equation 1. This change in TA was at or below the detection limit of current analytical methods (Ribas-Ribas et al., 2014). We therefore concluded that this potential artifact would not influence our carbonate-system calculations substantially. In contrast, the mean rate of change in DIC is 0.87 ± 1.02 μmol kg^{-1} y^{-1} or 16.53 μmol kg^{-1} over the 19 year period. Our analysis was consistent with spectrophotometric pH_T measurements carried out on three of our cruises and showed a decrease in pH_T with a mean rate of 0.0013±0.0009 units y^{-1}. This is consistent with other observations and estimates in the Atlantic Ocean which are in the range of -0.0017 to -0.0024 units y^{-1} (Bates, 2007; Bates et al., 2014; Lauvset and Gruber, 2014; Olafsson et al., 2009; Santana-Casiano et al., 2007). Previous studies reporting ocean acidification have largely focused on the North Atlantic Ocean and suggest higher acidification with increasing latitude. A further study, using 73 observations from the SOCAT v.2 fCO_2 database (www.socat.info), reported an acidification rate for the South Atlantic sub-tropical permanently stratified biome (represented by the SAG province here) of -0.0011 units y^{-1} for the period 1991-2011 (Lauvset et al., 2015).

Figure 7 shows pH_T trends for 5 different regions along the AMT transect: a) 25-38 ^oN (NAG: predominantly the North Atlantic Gyre); 8-20 ^oN (TUR: transitional region influenced by the wider Canary Current/Mauritanian/Guinea Dome upwelling systems); 1-8 ^oN (ITCZ: dominated by the Inter Tropical Convergence Zone); 1 ^oN-15 ^oS (Equ: dominated by the Equatorial Upwelling and South Equatorial Current) and 15-31 ^oS (SAG: South Atlantic Gyre). This figure shows some inter-hemispheric differences in the rates of ocean acidification with higher rates in the southern hemisphere, ITCZ and equatorial region. This is most pronounced in the NAG (25-38 ^oN) and SAG (15-31 ^oS) regions representing the oligotrophic subtropical gyres with average ocean acidification rates of -0.0009 and -0.0019 units y^{-1} respectively for our southbound cruises (Figure 7). This was somewhat surprising as we expected these two systems to show similar trends given their many other similarities (deep SML, persistent DCM and subsurface $O_{2\ max}$, oligotrophic nature). It is not clear whether this difference is genuinely interhemispheric or simply a reflection of season (boreal Autumn vs. austral Spring). Productivity in the oligotrophic, subtropical gyres is highest in Spring (Aiken et al., submitted; Smyth et al., submitted) and one may therefore expect to find higher pH_T during this period (owing to the uptake of CO_2 by primary producers). This

seasonality in productivity was also reflected in ΔfCO_2 with negative values suggesting net autotrophy and uptake of CO_2 (e.g. contrast for NAG-region between Figures 4 and 5). Indeed, during austral Spring, we observed higher pH_T for any given year in our time-series in the SAG (Figure 7) and concomitantly recorded predominantly negative ΔfCO_2, suggesting net autotrophy (Figure 4). Nevertheless, this does not explain the different ocean acidification rates in these biomes. The reasons for this are unclear in the absence of seasonally-resolved data, but add to the growing body of evidence which suggests that the two subtropical gyre biomes are biogeochemically distinct despite their many similarities (Baker and Jickells, submitted; Goetze et al., submitted; Moore et al., 2009; Moore et al., 2013; Serret et al., 2015).

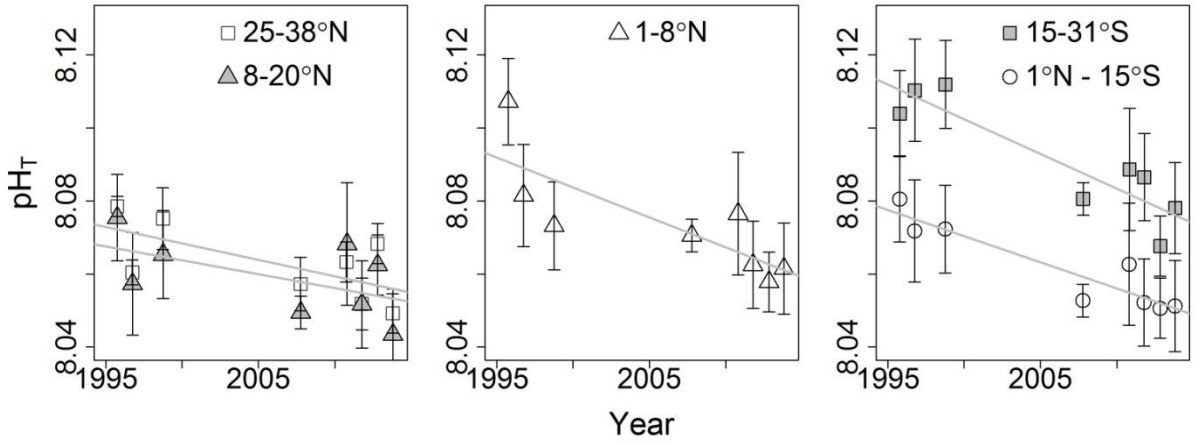

Figure 7: Average pH_T for five latitudinal provinces during southbound cruises: 25-38 ^{o}N (North Atlantic Gyre); 8-20 ^{o}N (transitional region influenced by the wider Canary Current/Mauritanian/Guinea Dome upwelling systems); 1-8 ^{o}N (dominated by the Inter Tropical Convergence); 1 ^{o}N-15 ^{o}S (dominated by the Equatorial Upwelling and South Equatorial Current) and 15-31 ^{o}S (South Atlantic Gyre). Error bars represent standard deviation of binned data over these latitudinal bands.

We also found ocean acidification for the regions which are influenced by upwelling systems (8-20 ^{o}N: Canary Current/Mauritanian/Guinea Dome and 1 ^{o}N-15 ^{o}S: Equatorial upwelling) (Figure 7). Conventional wisdom would suggest that regions where CO_2-rich deep-water is upwelled would be a source of CO_2 to the atmosphere and thereby not subject to ocean acidification. Whilst the former is clearly the case, as evidenced by positive ΔfCO_2 (Figures 4-5), the latter was not the case as OA was clearly observed (Figure 7). This is likely because as atmospheric CO_2 increases, the ΔfCO_2 is gradually decreasing (assuming constant CO_2 concentration in upwelled deep-waters). In turn, this would reduce the rate of CO_2

outgassing to the atmosphere, thus leading to retention of a higher proportion of deep water CO_2 in surface waters.

There is evidence to suggest that further ocean acidification may have an impact on biogeochemical cycles, including the C-cycle. In this issue, Tilstone et al. describe a set of 48-hour experiments investigating primary production under ocean acidification conditions (760 ppmv CO_2). These authors found an increase in photosynthetic rates at the lower pH, attributed primarily to dinoflagellates (Tilstone et al., submitted-b). Such short-term exposure experiments do not allow for genetic adaptation of the existing phytoplankton communities, but they nevertheless demonstrate the expected physiological response. If these finding are applicable at the basin scale, then primary production may increase under future OA. Indeed, an increase in microphytoplankton primary production from a 12-year time series of satellite ocean colour observations is reported for some regions of the Atlantic Ocean in this issue (Tilstone et al., submitted-a). Much of the work on ocean acidification has focused on calcification and calcifying organisms. For example a recent study of Antarctic pteropods living in low pH waters found that their shell thickness was significantly reduced when compared with the shells of their counterparts in higher pH water (Bednarsek et al., 2012). As yet, there is no evidence that pH is a major controlling variable in the biogeographic distribution of calcifying pteropods along the AMT track (Peijnenburg et al., in prep.). This apparent contrast may be reconciled by differences in the aragonite saturation state in different waters – shell thickness only decreases once the saturation state approaches unity or below. Other work has shown that calcification may be negatively impacted in some species and enhanced in others (Meyer and Riebesell, 2015). This is consistent with palaeontological records around the Palaeocene-Eocene thermal maximum which show a species succession over the transition to a lower-pH environment (O'Dea et al., 2014). Longer experiments have shown that calcifying coccolithophores may evolve and that calcification may recover over multiple generations of exposure to OA (Lohbeck et al., 2012). As pH decreases further, calcifying organisms may either adapt to OA by increasing their calcification rates or be replaced by others which are capable of higher calcification rates. However, studies on benthic calcifying organisms have shown that the energetic cost of increasing calcification comes at the expense of other metabolic processes in the long term (Wood et al., 2008).

Through the AMT programme, our study has quantified changes in surface ocean CO_2 and the carbonate system at the basin-scale. These changes are driven by the atmospheric increase of CO_2 and are superimposed on regional and seasonal cycles at present. However, the effect of long-term climatic cycles is unclear. This understanding requires further

sustained observations and is itself essential for the development of numerical models which can be used to predict the future impact of increasing atmospheric CO_2. We expect that novel technologies and further automation will make this task more cost-effective over the next two decades of AMT.

5. Acknowledgements

We would like to thank two anonymous reviewers for their constructive comments on this manuscript as well the officers and crew of the RRS James Clark Ross, Cook and Discovery for the successful delivery of the AMT programme. We would also like to thank the scientific personnel and principal scientists on our cruises for their support. Special thanks go to Dr. Andrew Rees for the coordination of AMT latterly as well as previous coordinators, Dr Carol Robinson and Prof. Jim Aiken. This study is a contribution to the international IMBER project and was supported by the UK Natural Environment Research Council National Capability funding, Greenhouse Gases Programme (grant no NE/K00249X/1), the European Commission (CARBOCHANGE, grant no 264879) and EU Horizons 2020 (AtlantOS, grant no 633211). This is AMT contribution no 300.

References

Aiken, J., Brewin, R.J.W., Dufois, F., Polimene, L., Hardman-Mountford, N., Jackson, T., Loveday, B., Mallor-Hoya, S., Dall'Olmo, G., Stephens, J., submitted. A synthesis of the North and South Atlantic Sub-Tropical Gyres and their response to environmental change during two decades of AMT. Progress in Oceanography this issue.

Anthony, K.R.N., Maynard, J.A., Diaz-Pulido, G., Mumby, P.J., Marshall, P.A., Cao, L., Hoegh-Guldberg, O., 2011. Ocean acidification and warming will lower coral reef resilience. Global Change Biology 17, 1798-1808.

Baker, A.R., Jickells, T.D., submitted. Atmospheric Deposition of Soluble Trace Elements along the Atlantic Meridional Transect (AMT). Progress in Oceanography this issue.

Bates, N.R., 2007. Interannual variability of the oceanic CO2 sink in the subtropical gyre of the North Atlantic Ocean over the last 2 decades. J. Geophys. Res.-Oceans 112.

Bates, N.R., Astor, Y.M., Church, M.J., Currie, K., Dore, J.E., Gonzalez-Davila, M., Lorenzoni, L., Muller-Karger, F., Olafsson, J., Magdalena Santana-Casiano, J., 2014. A Time-Series View of Changing Surface Ocean Chemistry Due to Ocean Uptake of Anthropogenic CO2 and Ocean Acidification. Oceanography 27, 126-141.

Beaufort, L., Probert, I., de Garidel-Thoron, T., Bendif, E.M., Ruiz-Pino, D., Metzl, N., Goyet, C., Buchet, N., Coupel, P., Grelaud, M., Rost, B., Rickaby, R.E.M., de Vargas, C., 2011. Sensitivity of coccolithophores to carbonate chemistry and ocean acidification. Nature 476, 80-83.

Bednarsek, N., Tarling, G.A., Bakker, D.C.E., Fielding, S., Jones, E.M., Venables, H.J., Ward, P., Kuzirian, A., Leze, B., Feely, R.A., Murphy, E.J., 2012. Extensive dissolution of live pteropods in the Southern Ocean. Nature Geoscience 5, 881-885.

Beman, J.M., Chow, C.-E., King, A.L., Feng, Y., Fuhrman, J.A., Andersson, A., Bates, N.R., Popp, B.N., Hutchins, D.A., 2011. Global declines in oceanic nitrification rates as a consequence of ocean acidification. Proceedings of the National Academy of Sciences of the United States of America 108, 208-213.

Bianchi, A.A., Bianucci, L., Piola, A.R., Pino, D.R., Schloss, I., Poisson, A., Balestrini, C.F., 2005. Vertical stratification and air-sea CO2 fluxes in the Patagonian shelf. J. Geophys. Res.-Oceans 110.

Broecker, W.S., Peng, T.H., 1974. Gas-Exchange Rates between Air and Sea. Tellus 26, 21-35.

Caldeira, K., Wickett, M.E., 2003. Anthropogenic carbon and ocean pH. Nature 425, 365-365.

Clayton, T.D., Byrne, R.H., 1993. Spectrophotometric seawater pH measurements - total hydrogen-ion concentration scale calibration of m-cresol purple and at-sea results. Deep-Sea Res. Part I-Oceanogr. Res. Pap. 40, 2115-2129.

Cooper, D.J., Watson, A.J., Ling, R.D., 1998. Variation of pCO_2 along a North Atlantic shipping route (UK to the Caribbean): A year of automated observations. Marine Chemistry 60, 147-164.

Curry, R., Mauritzen, C., 2005. Dilution of the northern North Atlantic Ocean in recent decades. Science 308, 1772-1774.

Dickson, A.G., 1990. Standard potential of the reaction -AgCl(s)+1/2H-2(g)=Ag(s)+HCl(aq) and the standard acidity constant of the ion HSO4- in synthetic sea-water from 273.15-K to 318.15-K. Journal of Chemical Thermodynamics 22, 113-127.

Dickson, A.G., Sabine, C.L., Christion, J.R., 2007. Guide to best practices for ocean CO_2 measurements. PICES Special Publication 3, PICES Special Publication 3, p. 191.

Duarte, C.M., Regaudie-de-Gioux, A., Arrieta, J.M., Delgado-Huertas, A., Agusti, S., 2013. The Oligotrophic Ocean Is Heterotrophic. Annual Review of Marine Science, Vol 5 5, 551-569.

Feely, R.A., Doney, S.C., Cooley, S.R., 2009. Ocean Acidification: Present Conditions and Future Changes in a High-CO2 World. Oceanography 22, 36-47.

Geider, R.J., 1987. Light and Temperature-dependence of the Carbon to Chlorophyll-a ratio in microalgae and cyanobacteria - implications for physiology and growth of phytoplankton. New Phytologist 106, 1-34.

Geider, R.J., MacIntyre, H.L., Kana, T.M., 1998. A dynamic regulatory model of phytoplanktonic acclimation to light, nutrients, and temperature. Limnology and Oceanography 43, 679-694.

Goetze, E., Hüdepohl, P.T., Chang, C., Van Woudenberg, L., Iacchei, M., Peijnenburg, K.T.C.A., submitted. Ecological dispersal barrier across the equatorial Atlantic in a planktonic copepod. Progress in Oceanography this issue.
Gonzalez-Davila, M., Magdalena Santana-Casiano, J., Ucha, I.R., 2009. Seasonal variability of fCO(2) in the Angola-Benguela region. Progress in Oceanography 83, 124-133.
Gruber, N., 1998. Anthropogenic CO2 in the Atlantic Ocean. Glob. Biogeochem. Cycle 12, 165-191.
Gruber, N., Keeling, C.D., Bates, N.R., 2002. Interannual variability in the North Atlantic Ocean carbon sink. Science 298, 2374-2378.
Hartmann, D.L., Klein-Tank, A.M.G., Rusticucci, M., Alexander, L.V., Brönnimann, S., Charabi, Y., Dentener, F.J., Dlugokencky, E.J., Easterling, D.R., Kaplan, A., Soden, B.J., Thorne, P.W., Wild, M., Zhai, P.M., 2013. Observations: Atmosphere and Surface, in: Stocker, T.F., D. Qin, Plattner, G.-K., Tignor, M., Allen, S.K., Boschung, J., Nauels, A., Xia, Y., Bex, V., Midgley, P.M. (Eds.), Climate Change 2013: The Physical Science Basis. Contribution of Working Group I to the Fifth Assessment Report of the Intergovernmental Panel on Climate Change. Cambridge University Press, Cambridge, United Kingdom and New York, NY, USA.
Hooker, S.B., Rees, N.W., Aiken, J., 2000. An objective methodology for identifying oceanic provinces. Progress in Oceanography 45, 313-338.
Johnson, Z.I., Wheeler, B.J., Blinebry, S.K., Carlson, C.M., Ward, C.S., Hunt, D.E., 2013. Dramatic Variability of the Carbonate System at a Temperate Coastal Ocean Site (Beaufort, North Carolina, USA) Is Regulated by Physical and Biogeochemical Processes on Multiple Timescales. Plos One 8.
Jones, E.M., Bakker, D.C.E., Venables, H.J., Watson, A.J., 2012. Dynamic seasonal cycling of inorganic carbon downstream of South Georgia, Southern Ocean. Deep-Sea Res. Part II-Top. Stud. Oceanogr. 59, 25-35.
Juranek, L.W., Quay, P.D., Feely, R.A., Lockwood, D., Karl, D.M., Church, M.J., 2012. Biological production in the NE Pacific and its influence on air-sea CO_2 flux: Evidence from dissolved oxygen isotopes and O_2/Ar. J. Geophys. Res.-Oceans 117.
Khatiwala, S., Tanhua, T., Fletcher, S.M., Gerber, M., Doney, S.C., Graven, H.D., Gruber, N., McKinley, G.A., Murata, A., Rios, A.F., Sabine, C.L., 2013. Global ocean storage of anthropogenic carbon. Biogeosciences 10, 2169-2191.
Kitidis, V., Hardman-Mountford, N.J., Litt, E., Brown, I., Cummings, D., Hartman, S., Hydes, D., Fishwick, J.R., Harris, C., Martinez-Vicente, V., Woodward, E.M.S., Smyth, T.J., 2012. Seasonal dynamics of the carbonate system in the Western English Channel. Continental Shelf Research 42, 30-40.
Kitidis, V., Laverock, B., McNeill, L.C., Beesley, A., Cummings, D., Tait, K., Osborn, M.A., Widdicombe, S., 2011. Impact of ocean acidification on benthic and water column ammonia oxidation. Geophysical Research Letters 38, doi: 10.1029/2011GL049095.
Lauvset, S.K., Gruber, N., 2014. Long-term trends in surface ocean pH in the North Atlantic. Marine Chemistry 162, 71-76.
Lauvset, S.K., Gruber, N., Landschuetzer, P., Olsen, A., Tjiputra, J., 2015. Trends and drivers in global surface ocean pH over the past 3 decades. Biogeosciences 12, 1285-1298.
Le Quéré, C., Moriarty, R., Andrew, R.M., Peters, G.P., Ciais, P., Friedlingstein, P., Jones, S.D., Sitch, S., Tans, P., Arneth, A., Boden, T.A., Bopp, L., Bozec, Y., Canadell, J.G., Chevallier, F., Cosca, C.E., Harris, I., Hoppema, M., Houghton, R.A., House, J.I., Jain, A., Johannessen, T., Kato, E., Keeling, R.F., Kitidis, V., Goldewijk, K.K., Koven, C., Landa, C.S., Landschützer, P., Lenton, A., Lima, I.D., Marland, G., Mathis, J.T., Metzl, N., Nojiri, Y., Olsen, A., Ono, T., Peters, W., Pfeil, B., Poulter, B., Raupach, M.R., Regnier, P., Rödenbeck, C., Saito, S., Salisbury, J.E., Schuster, U., Schwinger, J., Séférian, R., Segschneider, J., Steinhoff, T., Stocker, B.D., Sutton, A.J., Takahashi, T., Tilbrook, B., Werf, G.R.v.d., Viovy, N., Wang, Y.-P., Wanninkhof, R., Wiltshire, A., Zeng, N., 2015. Global carbon budget 2014 Earth System Science Data 7, 47-85.

Lee, K., Tong, L.T., Millero, F.J., Sabine, C.L., Dickson, A.G., Goyet, C., Park, G.H., Wanninkhof, R., Feely, R.A., Key, R.M., 2006. Global relationships of total alkalinity with salinity and temperature in surface waters of the world's oceans. Geophysical Research Letters 33, doi: 10.1029/2006gl027207.
Lefevre, N., 2009. Low CO2 concentrations in the Gulf of Guinea during the upwelling season in 2006. Marine Chemistry 113, 93-101.
Lefevre, N., Diverres, D., Gallois, F., 2010. Origin of CO2 undersaturation in the western tropical Atlantic. Tellus Series B-Chemical and Physical Meteorology 62, 595-607.
Lefevre, N., Moore, G., Aiken, J., Watson, A., Cooper, D., Ling, R., 1998. Variability of pCO2 in the Atlantic in 1995. Journal of Geophysical Research 100, 5623-5634.
Lefevre, N., Moore, G.F., 2000. Distribution of the CO2 partial pressure along an Atlantic Meridional transect. Progress in Oceanography 45, 401-413.
Lewis, E., Wallace, D.W.R., 1998. Program Developed for CO_2 System Calculations., ORNL/CDIAC-105. Carbon Dioxide Information Analysis Center, Oak Ridge National Laboratory, U.S. Department of Energy, Oak Ridge, Tennessee.
Lohbeck, K.T., Riebesell, U., Reusch, T.B.H., 2012. Adaptive evolution of a key phytoplankton species to ocean acidification. Nature Geoscience 5, 346-351.
Loucaides, S., Tyrrell, T., Achterberg, E.P., Torres, R., Nightingale, P.D., Kitidis, V., Serret, P., S.Woodward, E.M., Robinson, C., 2012. Biological and physical forcing of carbonate chemistry in an upwelling filament off northwest Africa: results from a Lagrangian study. Glob. Biogeochem. Cycle 26, GB3008.
Magdalena Santana-Casiano, J., Gonzalez-Davila, M., Ucha, I.R., 2009. Carbon dioxide fluxes in the Benguela upwelling system during winter and spring: A comparison between 2005 and 2006. Deep-Sea Res. Part II-Top. Stud. Oceanogr. 56, 533-541.
Marrec, P., Cariou, T., Collin, E., Durand, A., Latimier, M., Mace, E., Morin, P., Raimund, S., Vernet, M., Bozec, Y., 2013. Seasonal and latitudinal variability of the CO2 system in the western English Channel based on Voluntary Observing Ship (VOS) measurements. Marine Chemistry 155, 29-41.
Meyer, J., Riebesell, U., 2015. Reviews and Syntheses: Responses of coccolithophores to ocean acidification: a meta-analysis. Biogeosciences 12, 1671-1682.
Millero, F.J., Graham, T.B., Huang, F., Bustos-Serrano, H., Pierrot, D., 2006. Dissociation constants of carbonic acid in seawater as a function of salinity and temperature. Marine Chemistry 100, 80-94.
Moore, C.M., Mills, M.M., Achterberg, E.P., Geider, R.J., LaRoche, J., Lucas, M.I., McDonagh, E.L., Pan, X., Poulton, A.J., Rijkenberg, M.J.A., Suggett, D.J., Ussher, S.J., Woodward, E.M.S., 2009. Large-scale distribution of Atlantic nitrogen fixation controlled by iron availability. Nature Geoscience 2, 867-871.
Moore, C.M., Mills, M.M., Arrigo, K.R., Berman-Frank, I., Bopp, L., Boyd, P.W., Galbraith, E.D., Geider, R.J., Guieu, C., Jaccard, S.L., Jickells, T.D., La Roche, J., Lenton, T.M., Mahowald, N.M., Maranon, E., Marinov, I., Moore, J.K., Nakatsuka, T., Oschlies, A., Saito, M.A., Thingstad, T.F., Tsuda, A., Ulloa, O., 2013. Processes and patterns of oceanic nutrient limitation. Nature Geoscience 6, 701-710.
O'Dea, S.A., Gibbs, S.J., Bown, P.R., Young, J.R., Poulton, A.J., Newsam, C., Wilson, P.A., 2014. Coccolithophore calcification response to past ocean acidification and climate change. Nature Communications 5.
Olafsson, J., Olafsdottir, S.R., Benoit-Cattin, A., Danielsen, M., Arnarson, T.S., Takahashi, T., 2009. Rate of Iceland Sea acidification from time series measurements. Biogeosciences 6, 2661-2668.
Orr, J.C., Maier-Reimer, E., Mikolajewicz, U., Monfray, P., Sarmiento, J.L., Toggweiler, J.R., Taylor, N.K., Palmer, J., Gruber, N., Sabine, C.L., Le Quere, C., Key, R.M., Boutin, J., 2001. Estimates of anthropogenic carbon uptake from four three-dimensional global ocean models. Glob. Biogeochem. Cycle 15, 43-60.
Park, G.-H., Wanninkhof, R., 2012. A large increase of the CO2 sink in the western tropical North Atlantic from 2002 to 2009. J. Geophys. Res.-Oceans 117.
Perez, F.F., Rios, A.F., Roson, G., 1999. Sea surface carbon dioxide off the Iberian Peninsula (North Eastern Atlantic Ocean). J. Mar. Syst. 19, 27-46.

Rees, A.P., Robinson, C., Smyth, T., Aiken, J., Nightingale, P., Zubkov, M., 2015. 20 Years of the Atlantic Meridional Transect—AMT. Limnology and Oceanography Bulletin 24, 101-107.
Ribas-Ribas, M., Rérolle, V.M.C., Bakker, D.C.E., Kitidis, V., Lee, G.A., Brown, I., Achterberg, E.P., Hardman-Mountford, N.J., Tyrrell, T., 2014. Intercomparison of carbonate chemistry measurements on a cruise in northwestern European shelf seas. Biogeosciences 11, 4339-4355.
Riebesell, U., Schulz, K.G., Bellerby, R.G.J., Botros, M., Fritsche, P., Meyerhoefer, M., Neill, C., Nondal, G., Oschlies, A., Wohlers, J., Zoellner, E., 2007. Enhanced biological carbon consumption in a high CO2 ocean. Nature 450, 545-U510.
Santana-Casiano, J.M., Gonzalez-Davila, M., Rueda, M.J., Llinas, O., Gonzalez-Davila, E.F., 2007. The interannual variability of oceanic CO_2 parameters in the northeast Atlantic subtropical gyre at the ESTOC site. Glob. Biogeochem. Cycle 21.
Schuster, U., Watson, A.J., 2007. A variable and decreasing sink for atmospheric CO2 in the North Atlantic. J. Geophys. Res.-Oceans 112, doi: 10.1029/2006jc003941.
Schuster, U., Watson, A.J., Bates, N.R., Corbiere, A., Gonzalez-Davila, M., Metzl, N., Pierrot, D., Santana-Casiano, M., 2009. Trends in North Atlantic sea-surface fCO(2) from 1990 to 2006. Deep-Sea Res. Part II-Top. Stud. Oceanogr. 56, 620-629.
Serret, P., Robinson, C., Aranguren-Gassis, M., Elena Garcia-Martin, E., Gist, N., Kitidis, V., Lozano, J., Stephens, J., Harris, C., Thomas, R., 2015. Both respiration and photosynthesis determine the scaling of plankton metabolism in the oligotrophic ocean. Nature Communications 6.
Smyth, T., Quartly, G., Jackson, T., Tarran, G., Woodward, M., Harris, C., Gallienne, C., Thomas, R., Airs, R., Cummings, D., Brewin, R., Kitidis, V., Stephens, J., Zubkov, M., Rees, A., submitted. Determining Atlantic Ocean province variability. Progress in Oceanography this issue.
Tilstone, G., Lange, P.K., Misra, A., Brewin, R.J.W., Cain, T., submitted-a. Micro-phytoplankton photosynthesis, primary production and potential export production in the Atlantic Ocean. Progress in Oceanography this issue.
Tilstone, G., Šedivá, B., Tarran, G., Kaňa, R., Prášil, O., submitted-b. Effect of CO2 enrichment on phytoplankton photosynthesis in the North Atlantic sub-tropical gyre. Progress in Oceanography this issue.
Tilstone, G., Smyth, T., Poulton, A., Hutson, R., 2009. Measured and remotely sensed estimates of primary production in the Atlantic Ocean from 1998 to 2005. Deep-Sea Res. Part II-Top. Stud. Oceanogr. 56, 918-930.
Tilstone, G., Xie, Y., Robinson, C., Serret, P., Raitsos, D., Powell, T., Aranguren-Gassis, M., Garcia-Martin, E.E., Kitidis, V., 2015. Satellite estimates of net community production indicate predominance of net autotrophy in the Atlantic Ocean Remote Sensing of Environment 164, 254-269.
Wanninkhof, R., Doney, S.C., Bullister, J.L., Levine, N.M., Warner, M., Gruber, N., 2010. Detecting anthropogenic CO2 changes in the interior Atlantic Ocean between 1989 and 2005. J. Geophys. Res.-Oceans 115.
Weiss, R.F., 1974. Carbon dioxide in water and seawater: the solubility of a non-ideal gas. Marine Chemistry 2, 203-215.
Welshmeyer, N.A., 1994. Fluorometric analysis of chlorophyll a in the presence of chlorophyll b and phaeopigments. Limnology and Oceanography 39, 1985-1992.
Williams, P.J.l.B., Quay, P.D., Westberry, T.K., Behrenfeld, M.J., 2013. The Oligotrophic Ocean Is Autotrophic. Annual Review of Marine Science, Vol 5 5, 535-549.
Wood, H.L., Spicer, J.I., Widdicombe, S., 2008. Ocean acidification may increase calcification rates, but at a cost. Proceedings of the Royal Society B-Biological Sciences 275, 1767-1773.